Dynamic Traffic System Observability Problem

By

CHENLU PU

THESIS

Submitted in partial satisfaction of the requirements for the degree of

MASTER OF SCIENCE

in

Transportation Technology and Policy

in the

OFFICE OF GRADUATE STUDIES

of the

UNIVERSITY OF CALIFORNIA

DAVIS

Approved:

Yueyue Fan, Chair

H. Michael Zhang

Miguel A. Jaller Martelo

Committee in Charge

2021

Abstract

Real-time traffic information is crucial for traffic operations and management. Due to budget constraints, strategies for deploying sensors to effectively acquire the most critical information are desirable. While significant progress has been made on sensor location problem based on flow observability concept, most research on flow observability is based on static traffic data and only takes network topology into account. This thesis addresses the traffic network observability problem in a dynamic setting. Different from the observability concepts adopted for static settings, we consider all temporal and spatial relations of traffic flows to determine unobserved states. We first develop a state-space model to describe link density dynamics in virtue of a recently proposed link queue model. We then analyze the link queue model properties including phase transition, subspace boundary variation, and stability. Finally, based on full rank test or PBH test, we use examples to show critical network components where data need to be collected to ensure full network observability under different topology and congestion conditions.

Acknowledgements

I would like to firstly thank my supervisor, Prof. Yueyue Fan for her guidance and support no matter on research or life. She always encouraged me to think deeply and critically, although there is still a long way to go, it laid a good start for my future research. Her care for my life made me feel very warm especially under this terrible pandemic. I am so blessed to have her as my advisor, and I look forward to collaborating with her further in the future. Also, I would like to thank my thesis committee members, Prof. Michael Zhang, and Prof. Miguel Jaller for their suggestions and comments. Without their help, I could not complete this thesis.

I would like to thank my friends in Davis, Xinyue Hu, Xiaoyang Xue, Ning Liu, Ran Sun, Han Yang, and Yunteng Zhang for their company and support. I will never forget the scenery, the food, the festivals I enjoyed with Xinyue and Xiaoyang. I will never forget the insightful suggestions on my research from Ning Liu and Ran Sun. I will never forget the course ECI 016 I worked with Han Yang. I will never forget the encouragement from Yunteng Zhang. I also want to thank my friends in China, Yunshan Hu, Dan Zhao, Zijian Liu, Yukun Wang, and ATM team members for their online company. No matter how far apart we are, we will reunite one day.

Finally, I would like to express my deepest gratitude to my parents, E Zhao and Weijun Pu for their unconditional support and love. They treat me equally as an independent individual and give me enough respect, so I could develop my personality,

and choose my future. "Persevere and wait" is their only requirement of me, I will keep it in mind forever.

Contents

List of Figures

List of Tables

Chapter 1

Introduction

Information is indispensable in the transportation system, which improves traffic efficiency and safety by providing a basis for transportation planning in the long run and reflecting the current traffic condition for traffic monitoring, information service, traffic guidance, and so on in the short run.

Due to the budget constraint, it is impractical to put sensors everywhere to get enough information for system identification. How to obtain the system information as much as possible with the minimum budget for sensors attracts much attention from researchers during recent decades. To solve this problem, the concept of observability was firstly adopted by Castillo et al. (2008) and widely used by others in transportation system identification. Observability of the system is to measure how well the internal states could be identified by external outputs, which could be used as the objective of system information acquisition to deploy sensors. In the traffic system, flow information could be read directly by sensors or derived from relations, such as network topology and conservation law. The traffic flow observability aims to uniquely infer the unobserved flows by observed ones. In other words, based on observability analysis, we could determine the subset of flow information that need to be collected to obtain all flow information.

Currently, most of the state-of-the-art observability analysis in transportation lit-

erature is studied under a steady-state or in a static setting based on the null space method or network topological relations. Because the traffic condition is changing with time and traversing between stable and unstable phases back and forth, static observability conducted at a specific traffic condition is not enough to provide the optimal sensor location and then identify the whole system. Several studies employed the dynamic traffic model or other mathematical approaches to extend the observability in the dynamic setting. However, in these pieces of literature, linearization at the equilibrium point of the nonlinear traffic system constrains the scope of study space, the linearized system can not accurately describe the network traffic dynamics under unsteady states, employment of switching-mode model is plagued by the explosion of the number of subspaces, and there is no relevant research to analyze the properties of subspaces.

This thesis addresses the observability problem in the dynamical setting by using the link queue model proposed by Jin (2021) to approximate the nonlinear traffic system by a piecewise affine system, which extends the studied traffic network condition from a specific one (steady-state) to the whole state space. Instead of relying only on the network topological relationship, the paper also considers the traffic flow operational and temporal relations to infer unobserved link densities to achieve full observability. Specifically, properties including phase transition, subspace boundary variation, and stability of the link queue model are analyzed. Based on the proposed dynamic traffic system, full observability is analyzed under different network topology and congestion conditions for system identification.

The rest of the thesis is organized as follows. In Chapter 2, we review the related literature on dynamic traffic models and traffic observability problems, and the link queue model properties specifically. In Chapter 3, we display and analyze several properties of the link queue model and conduct observability analysis. In Chapter 4, we use several examples to show critical links where data need to be collected to ensure full network observability under different network congestion conditions and topologies.

In Chapter 5, we conclude this study with discussions, limitations, and future research topics.

Chapter 2

Literature Review

To address the dynamic observability problem, firstly, we need to select a proper dynamic traffic flow model to describe the traffic system, then solve the observability problem to identify the traffic system by relations like topology, conservation law, and so on. In this chapter, we reviewed the literature about dynamic traffic models and the observability problem in transportation, and layout the properties of the link queue model and reasons for selecting it.

2.1 Dynamic Traffic Flow Models Review

Dynamic traffic flow models used to describe the driver behaviors and explain the traffic phenomenon could be partitioned into deterministic models and stochastic ones.

2.1.1 Deterministic Models

According to different studied objectives, deterministic models could be classified into macroscopic models and microscopic models.

Macroscopic traffic flow models originated from the LWR model (Lighthill and Whitham (1955b), Lighthill and Whitham (1955a), Richards (1956)), which simulates traffic flows as continuous flows. Daganzo (1992, 1995) formulated the cell transmission

model (CTM) by discretizing the LWR model in space and time domains, which could describe the formation and propagation of flows under corridor case and three-legged junctions based on the triangular fundamental diagram. Various modifications of the CTM were proposed, like lagged cell transmission model (LCTM) in Daganzo (1999) and enhanced lagged cell transmission model (ELCTM) in Szeto (2008). To reduce the computation work, link-based models were proposed. Jin (2021) proposed the link queue model to enlarge the cell in CTM to link and treats vehicle accumulation on each link as a queue, in which link density dynamics is computed by in- and out-flux corresponding to ordinary, merging, and diverging junction rules. The model based on exit flow functions (MNO) is proposed by Merchant and Nemhauser (1978) to describe flow evolution on links, which yields the same result as the LWR model by refining the discretization of link length in Carey and McCartney (2004). For modeling the speed evolution with higher accuracy, additional higher-order terms were added in models proposed by Papageorgiou et al. (1990).

Microscopic models treat a single vehicle as the research object to study its trajectory and interaction with other vehicles, which includes the car-following model proposed by Newell (1993, 2002) and lane changing model by Gipps (1986).

2.1.2 Stochastic Models

In real life, various factors have an influence on traffic dynamics which includes weather, traffic facility, driver behavior, and so on. To better simulate the traffic dynamics, deterministic models are modified into stochastic ones.

In macroscopic models, Boel and Mihaylova (2006) and Sumalee et al. (2011) modified the CTM with stochastic demand and supply functions. However, modification of demand and supply functions could lead to negative densities, Jabari and Liu (2012) focused on the uncertainty on headway and could address this issue. Also, the stochastic higher-order continuum model based on the boltzmaan approach was proposed by

Prigogine and Andrews (1960).

In microscopic models, Markovian models and probabilistic cellular automation models are used to simulate the movement of an individual vehicle (Zhao and Spall (2018), Schreckenberg et al. (1995)). Compared with deterministic models, simulating stochastic Markovian models are more straightforward and faster. However, in the view of drivers, the stochastic model is unreasonable, because part of the driver's movement is determined in advance.

2.2 Reasons for Choosing Link Queue Models

This paper adopted the link queue model proposed by Jin (2021) to describe the dynamic traffic system because of the following properties:

(1) Compared with microscopic traffic models, the link queue model is a macroscopic model which describes the evolution of traffic flow rather than an individual vehicle. The studied parameter in the link queue model, link density, is the kind of information we want to acquire because this level of aggregated traffic condition can be directly used to support most traffic control strategies and it is readily obtainable by existing sensors deployed on roads.

(2) Based on the link queue model, the traffic system could be built easily in terms of conservation law, and we could directly use the definition of observability in control theory.

(3) Compared with the well-known LWR model, which is an infinite-dimensional PDE model, the link queue model is a finite-dimensional ODE model which enlarges the size of cells in the CTM to the link. The link queue model considers the traffic on each link as a queue that distributes uniformly on the link. Although it is too coarse for capturing the traffic dynamics on each link, it reduces the computation work efficiently by neglecting the difference of traffic condition for different locations on each link.

(4) Compared with exit flow models, which focus on more accurate exit flux functions,

the link queue model determines the in- and exit-flux functions by link densities and proper demand (supply) functions.

(5) The link queue model is a continuous approximation of kinematic wave models. Although shock waves and rarefaction waves cannot be captured in the link queue model, which are denoted by jumps of in- and exit flux function in kinematic wave models, the link queue model could exponentially approximate the transition of these jumps, which could be considered as continuous shock waves and rarefaction waves.

2.3 Review of Observability

In transportation, the flow observability problem studies whether there exists a unique solution of the flow conservation equation, or how to select the observable information to uniquely identify the whole traffic system. Based on the flow observability, we can deploy the sensors to obtain the most information of interest.

2.3.1 Static Observability

Most of the studies are based on static or steady-state traffic. Castillo et al. (2015) and Gentili and Mirchandani (2012) provided state-of-the-art reviews of the sensor location method, in which the observability problem is also discussed in detail.

The static observability problem could be classified by categories of traffic flow as link flow observability, OD flow observability, and path flow observability, and general flow observability.

For link flow observability, methods could be further subdivided into OD-based approaches, node-based approaches, path-based approaches, and graphical approaches. Based on the link-OD incidence matrix, Castillo et al. (2008) proposed the nullspace method to uniquely determine the unobserved flow. Based on the link-path incidence matrix, a reduced row echelon form (RREF) method is proposed for path-based observability by Hu et al. (2009). Path enumeration is required for path-based observability,

which is infeasible for large-scale networks. Therefore, a node-based approach based on flow conservation law is proposed for full link flow observability by Ng (2012). Based on graph theory, the spanning tree method was firstly suggested by Mori and Tsuzuki (1991) in power system observability and used by He (2013) to solve the link flow observability in virtue of a virtue node and virtue links to reproduce node inflows and outflows. If the system wants to achieve full observability, at least 60-70 percent of links need to be equipped with counting sensors (Hu et al. (2009); Ng (2012); He (2013); Castillo et al. (2013)), optimal partial observability solution is proposed by Viti et al. (2014).

For OD, path, and general flow observability, information from counting sensors is limited in that counting data is not sufficient to identify OD and path flow. Therefore, the plate scanning technique is introduced to provide the OD and path flows. Castillo et al. (2012) proposed a method of measuring information (FAO), and determined the minimal set of links to be scanned for full observability of all flows (link, OD, path).

2.3.2 Dynamic Observability

Recently, observability is analyzed in dynamic traffic system setting to gain more real-time information.

A switching-mode model based on the cell transmission model is proposed by Muñoz et al. (2003) to estimate traffic densities only for the corridor case, in which the observability and controllability properties of each switching mode are summarized to advise sensor location. Agarwal et al. (2016) formulated a state-space model based on the ordinary differential equation setting to describe the network routing dynamics at the node and density dynamics on the link. Then observability is analyzed at the equilibrium point of the linearized system, which only holds for a certain network condition. Rostami-Shahrbabaki et al. (2020) formulated a two-layer model for traffic flow evolution based on connected vehicle data to transform the inherently switching

nonlinear system into a non-switching linear-in-parameters one and employed a graphical approach proposed by Liu et al. (2013) to find the optimal sensor location for full observability of link densities. Compared with other methods, using connected vehicle data could efficiently reduce the number of or even without counting sensors to estimate all link densities. Nevertheless, the penetration of connected vehicles will influence the accuracy, and the graphical approach is necessary and generally not sufficient for the full observability of an arbitrary network. Moreover, the two-layer model underestimates link densities for the no queue case and overestimates link densities for the spillback case.

Chapter 3

Methodologies

This chapter firstly reviews the link queue model and rewrites it as a piecewise affine system based on the triangular fundamental diagram. Then based on the simplest two-link network, we show some properties of the link queue model, including phase transition, subspace boundary variation, and stability. Finally, we introduce the definition of observability in the dynamical system and show the full rank test and Popov-Belevitch-Hautus (PBH) test.

3.1 Preliminaries of the Link Queue Model

3.1.1 The Link Queue Model Review

According to flow conservation law, the classic macroscopic traffic flow model, the LWR model (Lighthill and Whitham (1955b), Lighthill and Whitham (1955a), Richards (1956)) treats traffic flows as continuous flows and formulates the relationship between traffic density and flux in a partial differential equation given by (3.1), in which $k(x,t)$ denotes the traffic density of location x at time t, $q(x,t)$ denotes the flux of location x at time t.

$$\frac{\partial k(x,t)}{\partial t} + \frac{\partial q(x,t)}{\partial x} = 0 \tag{3.1}$$

For the sake of simplification and reduce the computation work, Jin (2021) assumed that traffic on the link is homogeneous and treated traffic as a queue on each link, then proposed the link queue model which transforms the LWR model from PDE model to the ODE model. The flow conservation on normal links is shown as (3.2), where $k_a(t)$ denotes the average link density of link a at time t, $f_a(t)$ denotes the influx of link a at time t, $g_a(t)$ denotes the outflux of link a at time t, L_a denotes the length of link a, Δ denotes the set of directed links in the studied traffic network.

$$\dot{k}_a(t) = \frac{f_a(t) - g_a(t)}{L_a}, \forall a \in \Delta \tag{3.2}$$

In order to solve the equation (3.2), demand and supply functions are introduced as (3.3a) and (3.3b) to relate the inflow and outflow of each link with link densities. In euqation (3.3), $d_a(t)$ and $s_a(t)$ denote the demand and supply flow of link a at time t respectively, $Q_a(k_a(t))$ denotes a unimodal function of traffic flow in link density k_a, C_a denotes the capacity of link a attained at critical density $k_{a,c}(Q_a(k_{a,c}) = C_a \geq Q_a(k_a))$.

$$d_a(t) = \begin{cases} Q_a(k_a(t)), \text{ if not congested}(k_a(t) < k_{a,c}) \\ C_a, \text{ if congested}(k_a(t) \geq k_{a,c}) \end{cases} \tag{3.3a}$$

$$s_a(t) = \begin{cases} C_a, \text{ if not congested}(k_a(t) < k_{a,c}) \\ Q_a(k_a(t)), \text{ if congested}(k_a(t) \geq k_{a,c}) \end{cases} \tag{3.3b}$$

The formulation of demand and supply functions are intuitively understandable. The demand function describes the relationship between sending flow from the current link to the downstream link and current link density, which increases with density if the current link density less than critical density and stays at the capacity level otherwise. When the link density is bigger than the critical density, the queue begins to form and flows out at the maximum rate, like the situation that the traffic light turns to green

from red. Similarly, the supply function describes the relationship between receiving flow from the upstream link to the current link and current link density, which decreases with increasing density if the current link density is bigger than critical density and stays at the capacity level otherwise, that is because the queue in the present link will occupy some space and influence the receiving flow.

The function of inflow (outflow) regarding demand and supply of each link is formulated as (3.4), which under node flow conservation law and could track the direction of flow propagation. At a junction $j \in J$, $\boldsymbol{g_j(t)}$ denotes the vector of the outflow of upstream links of junction j, $\boldsymbol{f_j(t)}$ denotes the vector of the outflow of downstream links of junction j, $\boldsymbol{d_j(t)}$ denotes the vector of upstream demands of junction j, $\boldsymbol{g_j(t)}$ denotes the vector of the outflow of downstream supplies of junction j.

$$(\boldsymbol{g_j(t)}, \boldsymbol{f_j(t)}) = \mathbb{FF}(\boldsymbol{d_j(t)}, \boldsymbol{s_j(t)}) \tag{3.4}$$

Equation (3.4) is consistent with macroscopic flow behaviors at three types of junctions, which guarantees the convergence to the LWR model and determines the unique solution of equation (3.2) in Jin (2017). To reduce categories of junctions, we consider the following three types: ordinary, merging, and diverging. In practical traffic network, to avoid the conflict of flows of different directions, most networks could be reconstructed by these three junctions. Three types of junctions are shown as Figure 3.1. Flux functions not only reflects the practical flow dynamics on all three types of junctions but also under several constraints:

(1) Flow conservation at each junction;

(2) The influx of each link is not greater than its supply and upstream demand;

(3) The outflux of each link is not greater than its demand and downstream supply;

(4) The flux function should be invariant (Jin (2017)).

Ordinary Junction

Ordinary junction is depicted in Figure 3.1 on the left. The function of the outflux

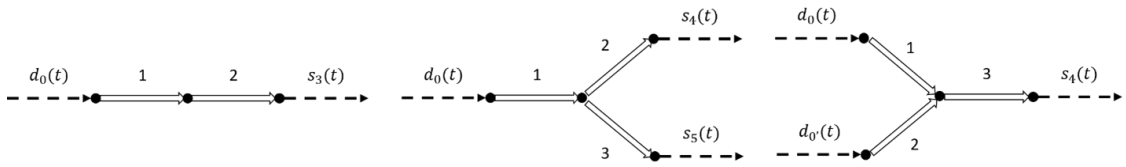

Figure 3.1: Three types of junctions, from left to right are ordinary, diverging, and merging

of upstream link equals that of influx of downstream link in (3.4) are formulated as equation (3.5).

$$g_1(t) = f_2(t) = \min\{d_1(t), s_2(t)\} \tag{3.5}$$

Diverge Junction

Diverge junction is depicted in Figure 3.1 in the middle. According to the first-in-first-out diverging rule and known split ratio, functions of ourflux and influx are defined as (3.6), where $\xi_{1\to2}(t)$ denotes the ratio of the number of vehicles advancing from link 1 to 2 to the total number of vehicles passing junction j.

$$g_1(t) = \min\left\{d_1(t), \frac{s_2(t)}{\xi_{1\to2}(t)}, \frac{s_3(t)}{\xi_{1\to3}(t)}\right\}, \tag{3.6a}$$

$$f_2(t) = \xi_{1\to2}(t)g_1(t), \tag{3.6b}$$

$$f_3(t) = \xi_{1\to3}(t)g_1(t). \tag{3.6c}$$

Merge Junction

Merge junction is depicted in Figure 3.1 on the right. Functions of outflux of upstream links in (3.4) are defined as (3.7b, c) by fair merging rule, the function of the influx of the downstream link in (3.4) is defined as (3.7a).

$$f_3(t) = \min\left\{d_1(t) + d_2(t), s_3(t)\right\}, \tag{3.7a}$$

$$g_1(t) = \min\left\{d_1(t), \max\left\{s_3(t) - d_2(t), \frac{C_1}{C_1 + C_2}s_3(t)\right\}\right\}, \tag{3.7b}$$

$$g_2(t) = f_3(t) - g_1(t). \tag{3.7c}$$

3.1.2 Triangular Fundamental Diagram-Based Link Queue Model

To extend the studied network statuses from steady state to all states, we choose the triangular fundamental diagram to formulate a switched linear dynamic system instead of following the path of linearizing the nonlinear system based on Greenshields' model at the steady state. The triangular fundamental diagram of link a is shown in Figure 3.2, the corresponding flow, demand, and supply function are defined as (3.8) respectively, where v_a denotes the free flow speed of link a (the slope of increasing part in blue), w_a denotes the speed of backward shock wave on link a (the slope of decreasing part in orange), $k_{a,c}$ denotes the critical link density of link a, $k_{a,j}$ denotes the jam density of link a.

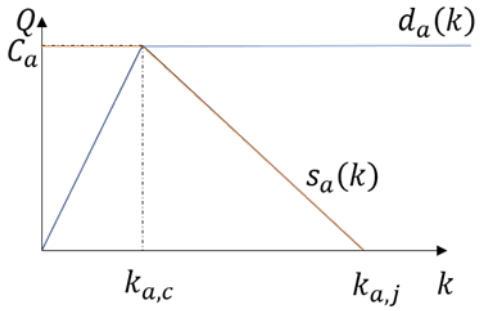

Figure 3.2: Triangular fundamental diagram and corresponding demand and supply function

$$Q_a(t) = \min\{v_a k_a(t), -w_a k_a(t) + (\frac{w_a}{v_a} + 1)C_a\}, \tag{3.8a}$$

$$d_a(t) = \min\{v_a k_a(t), C_a\}, \tag{3.8b}$$

$$s_a(t) = \min\{-w_a k_a(t) + (\frac{w_a}{v_a} + 1)C_a, C_a\} \tag{3.8c}$$

Bringing the piecewise linear demand (supply) function in influx (outflux) function, and then in equation (3.2), we obtain the piecewise affine system as equation (3.9a, b)

to describe traffic dynamics considering all traffic conditions:

$$\dot{\boldsymbol{K}}(t) = \boldsymbol{A_i}\boldsymbol{K}(t) + \boldsymbol{b_i}, if\ \boldsymbol{K}(t) \in \boldsymbol{R_i}, \boldsymbol{R_i} = \{\boldsymbol{K}(t)|\boldsymbol{E_i}\boldsymbol{K}(t) + \boldsymbol{e_i} \leq \boldsymbol{0}\}, \tag{3.9a}$$

$$\boldsymbol{Y}(t) = \boldsymbol{C}\boldsymbol{K}(t) \tag{3.9b}$$

Based on the link queue model proposed by Jin (2021) and triangular fundamental diagram, we could rewrite the network flow conservation equations into general form of linear system shown in (3.9a), which is also known as transition equation. The transition equation of each subspace is shown in (3.9a), where $\boldsymbol{K}(t) \in \mathbb{R}^n$ denotes the vector of link densities at time t, $\boldsymbol{A_i} \in \mathbb{R}^{n \times n}$ denotes the transition matrix corresponding to the ith subspace, $\boldsymbol{b_i}(t) \in \mathbb{R}^n$ denotes the vector of constant term corresponding to the ith subspace at time t. The studied space of the piecewise affine system consists of n dimensions, each dimension measures the density of one link, which satisfies the constraints $k_a(t) \in [0, k_{a,j}(t)], \forall a \in \Delta$. Because of the Min operator in demand (supply) and influx (outflux) function, there exists some switching points in demand (supply) and influx (outflux) functions. The sets of switching points make up boundaries which divide the whole studied space into subspaces. Each element of the Min operator is linear, therefore each subspace is a linear system. $\boldsymbol{R_i} = \{\boldsymbol{K}(t)|\boldsymbol{E_i}\boldsymbol{K}(t) + \boldsymbol{e_i} \leq \boldsymbol{0}\}$ denotes the ith subspace, that is the ith closed convex polyhedral. The measurement equation of each subspace is shown in (3.9b), where $\boldsymbol{Y}(t) = \boldsymbol{C}\boldsymbol{K}(t)$ denotes the vector of output, in other words, observed link densities at time t, $\boldsymbol{C}$ denotes the measurement matrix, indicating which link could be observed and the location of sensors.

3.2 Properties of the Link Queue Model

3.2.1 Subspaces and Phase Transition

For simplicity, the ordinary two-link case as an example is shown to display the piecewise affine system. The two-link network with demand $d_0(t)$ and supply $s_3(t)$ is shown in Figure 3.3.

Given the condition that demand and supply as $d_0(t) = 2340veh/h$, $s_3(t) = 1170veh/h$, link capacities as $C_1 = 4680veh/h$, $C_2 = 2340veh/h$, free flow speed as $v_1 = v_2 = 65km/h$, backward shock wave speed as $w_1 = w_2 = 16.25km/h$, and length of two links are 1 km, there are total 8 subspaces in the feasible space. Each subspace corresponds to a distinct network congestion status in real life. In each subspace, the transition equation is unchanged, that is, the influx and outflux function of each link is fixed, the dynamics of traffic are homogeneous. The transition equation, corresponding transition matrix, and eigenvalues of the transition matrix of eight subspaces are shown in Table 3.1.

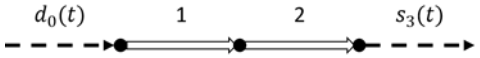

Figure 3.3: Two-link network

Table 3.1: Transition equation of each subspace of two-link network

Index	Transition equation	Transition matrix	Eigenvalues
1	$\dot{k}_1 = d_0 - v_1 k_1$ $\dot{k}_2 = v_1 k_1 - v_2 k_2$	$\begin{bmatrix} -v_1 & 0 \\ v_1 & -v_2 \end{bmatrix}$	$-v_1, -v_2$
2	$\dot{k}_1 = -w_1 k_1 + (\frac{w_1}{v_1} + 1)C_1$ $-(-w_2 k_2 + (\frac{w_2}{v_2} + 1)C_2)$ $\dot{k}_2 = -w_2 k_2 + (\frac{w_2}{v_2} + 1)C_2 - s_3$	$\begin{bmatrix} -w_1 & w_2 \\ 0 & -w_2 \end{bmatrix}$	$-w_1, -w_2$
3	$\dot{k}_1 = -w_1 k_1 + (\frac{w_1}{v_1} + 1)C_1 - C_2$ $\dot{k}_2 = C_2 - v_2 k_2$	$\begin{bmatrix} -w_1 & 0 \\ 0 & -v_2 \end{bmatrix}$	$-w_1, -v_2$

4	$\dot{k}_1 = d_0 - v_1 k_1$ $\dot{k}_2 = v_1 k_1 - s_3$	$\begin{bmatrix} -v_1 & 0 \\ v_1 & 0 \end{bmatrix}$	$0, -v_1$
5	$\dot{k}_1 = d_0 - (-w_2 k_2 + (\frac{w_2}{v_2} + 1)C_2)$ $\dot{k}_2 = -w_2 k_2 + (\frac{w_2}{v_2} + 1)C_2 - s_3$	$\begin{bmatrix} 0 & w_2 \\ 0 & -w_2 \end{bmatrix}$	$0, -w_2$
6	$\dot{k}_1 = d_0 - C_2$ $\dot{k}_2 = C_2 - v_2 k_2$	$\begin{bmatrix} 0 & 0 \\ 0 & -v_2 \end{bmatrix}$	$0, -v_2$
7	$\dot{k}_1 = -w_1 k_1 + (\frac{w_1}{v_1} + 1)C_1 - C_2$ $\dot{k}_2 = C_2 - s_3$	$\begin{bmatrix} -w_1 & 0 \\ 0 & 0 \end{bmatrix}$	$0, -w_1$
8	$\dot{k}_1 = d_0 - C_2$ $\dot{k}_2 = C_2 - s_3$	$\begin{bmatrix} 0 & 0 \\ 0 & 0 \end{bmatrix}$	$0, 0$

Above 8 subspaces are shown in Figure 3.4 by phase portrait with labels corresponding to index in Table 3.1. Setting the initial condition as $k_1(0) = k_2(0) = 0$ and solving the two link network piecewise affine system above numerically, the trajectory of the solution is sketched in Figure 3.4 in black. The trajectory starts at the origin and ends at $k_1 = 288veh/km$, $k_2 = 108veh/km$ after passing through 4 subspaces, index as 1-4-5-2 shown in Table 3.1 in order. The density, influx, and outflux of each link changes with time are shown in Figure 3.5, in which phase 1-2-3-4 corresponding to 4 subspaces in order.

The first subspace the trajectory traverses in blue in Figure 3.4, refers to light traffic condition with increasing outflux for all links and the fixed influx of link 1 which equals to d_0 shown in Figure 3.5, the traffic rarefaction wave begins to form at the start point of link 1 and reach the end of link 2.

The second subspace the trajectory traverses in gold in Figure 3.4, refers to light traffic condition with fixed outflux of link 2 which equals to s_3 shown in Figure 3.5,

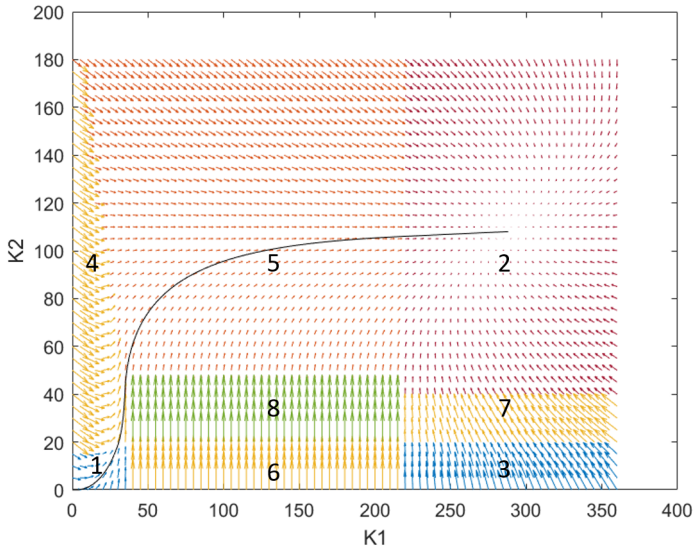

Figure 3.4: Phase portrait and a trajectory start from origin

the number of vehicles on the network continues to increase.

The third subspace the trajectory traverses in orange in Figure 3.4, refers to light traffic on link 1 and congestion on link 2 with decreasing influx of link 2 (outflux of link 1) shown in Figure 3.5. The queue begins to form on link 2 and propagate backward to upstream.

The fourth subspace the trajectory traverses in red in Figure 3.4, refers to congestion on both links with decreasing influx of link 1 shown in Figure 3.5. There is no additional space on link 2 and queue begins to form on link 1 and propagate backward to upstream until both links are totally congested.

3.2.2 Variation of Subspace Boundaries

Subspaces in the studied state space are disjoint, so the boundaries between different subspaces are explicit and could be expressed by linear equations. The related variables of boundaries are demand d_0, supply s_3, and link capacities C_1, C_2. In this part, we analyze the influence of 4 variables on the variation of boundaries one by one. The number of subspaces is changing with mentioned 4 parameters. Some of the sub-

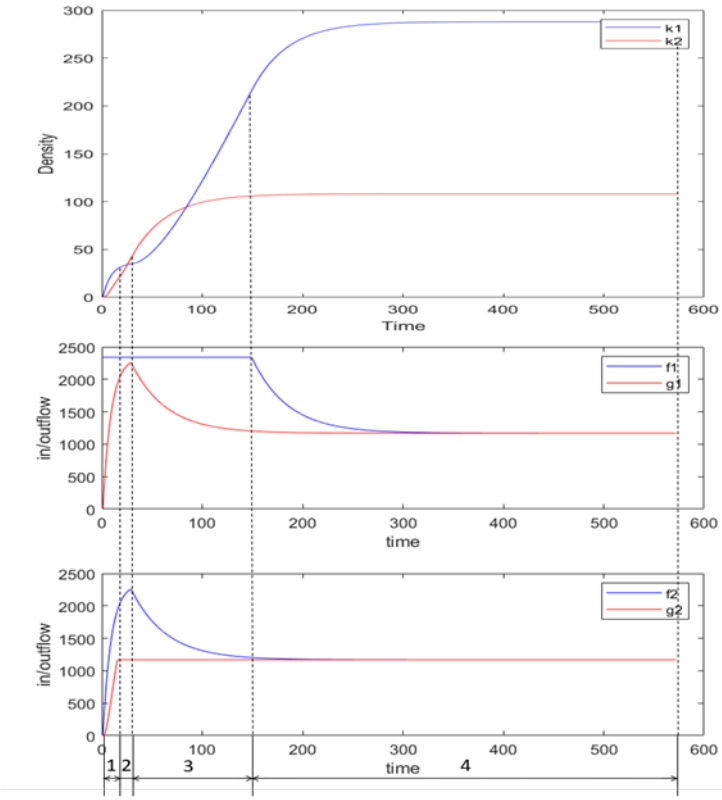

Figure 3.5: Density vs. Time and inflow(outflow) vs. time

spaces exist in the whole range of the parameter space, however, others disappear in certain ranges of the parameter space. Most of the time, there are total 8 subspaces. When $d_0(t) = 2340veh/h$, $s_3(t) = 1170veh/h$, $C_1 = 4680veh/h$, $C_2 = 2340veh/h$, $v_1 = v_2 = 65km/h$, $w_1 = w_2 = 16.25km/h$, the whole state space is divided by 5 straight lines into 8 subspaces shown in Figure 3.6.

In Figure 3.6, two lines in black are the boundaries of state spaces, line 1 is $k_1 = k_{1,j}$, line 2 is $k_2 = k_{2,j}$, line 3 in magenta is $v_2k_2 = s_3$, line 4 in red is $-w_2k_2 + (\frac{w_2}{v_2} + 1)C_2 = C_2$, line 5 in cyan is $v_1k_1 = C_2$, line 6 in blue is $-w_1k_1 + (\frac{w_1}{v_1} + 1)C_1 = d_0$, line 7 in green is $v_1k_1 = -w_2k_2 + (\frac{w_2}{v_2} + 1)C_2$. The label of subspaces in Figure 3.6 is accord with that in Table 3.1, and Figure 3.4.

If we fix the other three parameters and only change d_0 from $0veh/h$ to $4680veh/h$, the variation of boundaries is shown in Figure 3.7 on the left. We can find that only the plane in blue is not orthogonal to k1-k2 plane, so the boundary in blue is moving to

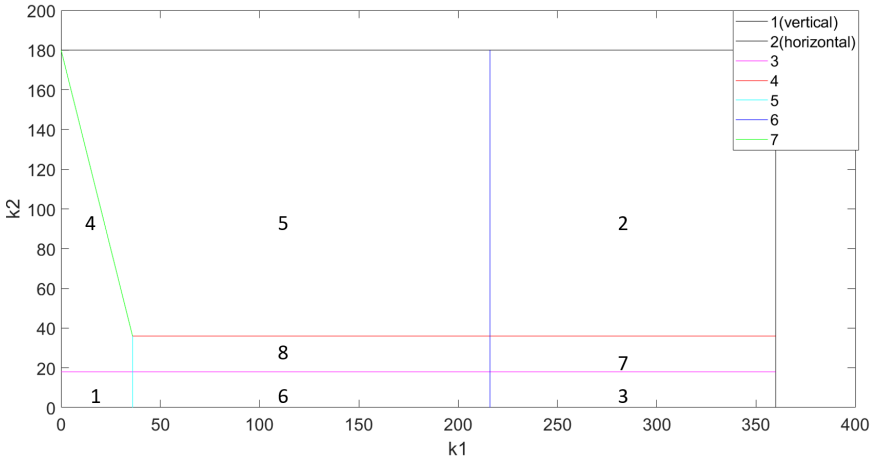

Figure 3.6: Subspaces and boundaries

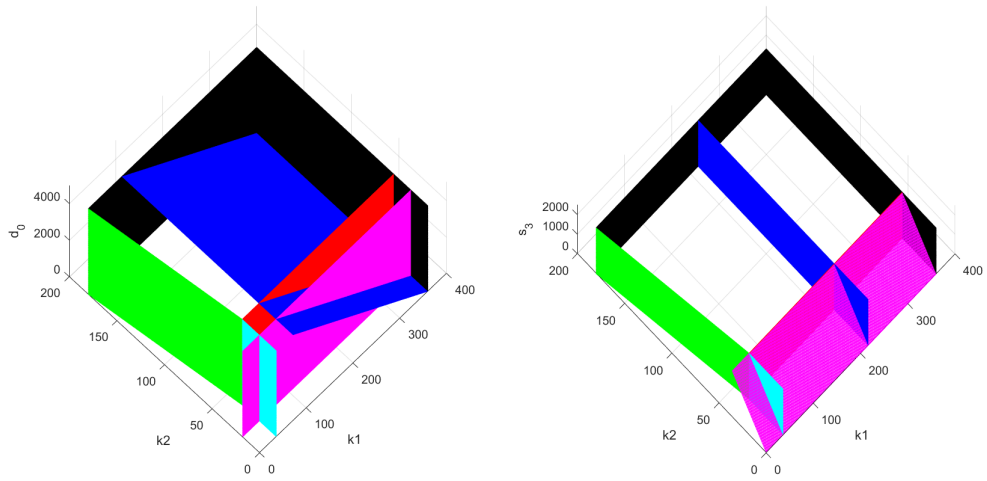

Figure 3.7: Boundaries variation with changing d_0 only on the left and changing s_3 only on the right

the bottom left as the demand d_0 increases. In addition, when $d_0 = 0veh/h$, the 2nd, 3rd and 7th subspaces disappear and there are a total of 5 subspaces. As d_0 reaches 4680 veh/h and continues increasing, the boundary in blue stops moving to the left, and the expression is changed to $-w_1k_1 + (\frac{w_1}{v_1} + 1)C_1 = C_1$. Moreover, the 1st, 4th, 5th, 6th and 8th subspaces are replaced by the following subspaces in Table 3.2.

Table 3.2: Replaced subspaces and their substitutes

Index	Replaced transition equation	Index	New transition equation
1	$\dot{k}_1 = d_0 - v_1k_1$ $\dot{k}_2 = v_1k_1 - v_2k_2$	1'	$\dot{k}_1 = C_1 - v_1k_1$ $\dot{k}_2 = v_1k_1 - v_2k_2$
4	$\dot{k}_1 = d_0 - v_1k_1$ $\dot{k}_2 = v_1k_1 - s_3$	4'	$\dot{k}_1 = C_1 - v_1k_1$ $\dot{k}_2 = v_1k_1 - s_3$
5	$\dot{k}_1 = d_0 - (-w_2k_2 + (\frac{w_2}{v_2} + 1)C_2)$ $\dot{k}_2 = -w_2k_2 + (\frac{w_2}{v_2} + 1)C_2 - s_3$	5'	$\dot{k}_1 = C_1 - (-w_2k_2 + (\frac{w_2}{v_2} + 1)C_2)$ $\dot{k}_2 = -w_2k_2 + (\frac{w_2}{v_2} + 1)C_2 - s_3$
6	$\dot{k}_1 = d_0 - C_2$ $\dot{k}_2 = C_2 - v_2k_2$	6'	$\dot{k}_1 = C_1 - C_2$ $\dot{k}_2 = C_2 - v_2k_2$
8	$\dot{k}_1 = d_0 - C_2$ $\dot{k}_2 = C_2 - s_3$	8'	$\dot{k}_1 = C_1 - C_2$ $\dot{k}_2 = C_2 - s_3$

Similarly, if we only change s_3 from $0veh/h$ to $2340veh/h$, the variation of boundaries is shown in Figure 3.7 on the right. Except for the plane in magenta, other planes are orthogonal to the k1-k2 plane, so the boundary in magenta is moving to the upper left as the supply s_3 increases. In addition, when $s_3 = 0veh/h$, the 1st, 3rd and 6th subspaces disappear, and there are a total of 5 subspaces. When $s_3 = 2340veh/h$, the boundary in magenta and that in red coincide with each other at the line $-w_2k_2 + (\frac{w_2}{v_2} + 1)C_2 = C_2$, 7th and 8th subspaces disappear and there are 6 subspaces in total.

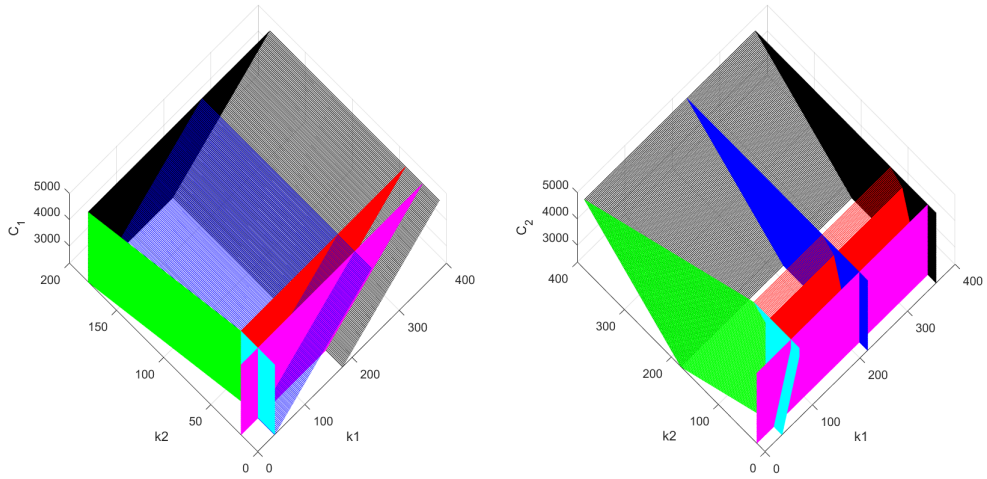

Figure 3.8: Boundaries variation with changing C_1 only on the left and changing C_2 only on the right

If we choose link 1 capacity C_1 as the only variable and change it from $2340veh/h$ to $5000veh/h$, the variation of boundaries is shown in Figure 3.8 on the left. Using the same method described above, we can find the boundary in bule and the boundary of k_1 are moving to the upper right with the increasing C_1. Besides, when $C_1 = 2340veh/h$, the boundary in cyan overlaps a part of the boundary in blue, the 6th and 8th subspaces disappear and there are 6 subspaces in total.

If we choose link 2 capacity C_2 as the only variable and change it from $2340veh/h$ to $5000veh/h$, the variation of boundaries is shown in Figure 3.8 on the right. In the same way, we can find the boundary in bule, in magenta, and the boundary of k_1 is fixed and other boundaries are moving with the increasing C_2. After C_2 reaching C_1 and continuing increasing, the boundary in cyan is changed from $v_1k_1 = C_2$ to $v_1k_1 = C_1$ and fixed at this line, the movement speed of the boundary in red increases as well. Moreover, when $C_2 > C_1$, the 3rd, 6th, 7th and 8th subspaces are replaced by other subspaces displayed in Table 3.3. However, no matter how we change the C_2, the number of subspaces is always 8.

Table 3.3: Replaced subspaces and their substitutes

Index	Replaced transition equation	Index	New transition equation
3	$\dot{k}_1 = -w_1k_1 + (\frac{w_1}{v_1} + 1)C_1 - C_2$ $\dot{k}_2 = C_2 - v_2k_2$	3"	$\dot{k}_1 = -w_1k_1 + (\frac{w_1}{v_1} + 1)C_1 - C_1$ $\dot{k}_2 = C_1 - v_2k_2$
6	$\dot{k}_1 = d_0 - C_2$ $\dot{k}_2 = C_2 - v_2k_2$	6"	$\dot{k}_1 = d_0 - C_1$ $\dot{k}_2 = C_1 - v_2k_2$
7	$\dot{k}_1 = -w_1k_1 + (\frac{w_1}{v_1} + 1)C_1 - C_2$ $\dot{k}_2 = C_2 - s_3$	7"	$\dot{k}_1 = -w_1k_1 + (\frac{w_1}{v_1} + 1)C_1 - C_1$ $\dot{k}_2 = C_1 - s_3$
8	$\dot{k}_1 = d_0 - C_2$ $\dot{k}_2 = C_2 - s_3$	8"	$\dot{k}_1 = C_1 - C_2$ $\dot{k}_2 = C_2 - s_3$

According to the above four experiments, we can find that besides boundaries are moving with changes in parameters, the configuration of the whole space is changing as well, some subspaces appear or disappear for a certain range of parameters. In addition, with changes in parameters, the vector field is affected as well, the trajectory of the solution may pass through different subspaces, but it will definitely end at the equilibrium point, so subspaces containing the equilibrium point which is defined as stable subspaces are more crucial for us to consider. As the network topology becomes more and more complex, the number of subspaces will explode. It is impractical to consider all subspaces in that not all subspaces will occur simultaneously and the importance of subspaces are different as well. Considering the practical range of parameters, and the equilibrium analysis discussed in the following section, we could determine the stable subspaces and select the subspaces of interest to conduct observability analysis, which is helpful for sensor deployment.

3.2.3 Stability

Stability is an important property studied in a dynamical system, which describes the stability and recovery of trajectories of dynamical systems under small perturbations of initial conditions. Compared with transient unstable states, stable equilibrium could recover itself, like the simple gravity pendulum, which is always back to the equilibrium position no matter where to release it. For the piecewise affine system, only equilibriums within corresponding subspaces are valid as sinks to attract trajectories. Therefore, in this section, we firstly introduce the related definitions of stability, then determine stable equilibrium points and conditions of them within corresponding subspaces.

Definition(Hirsch (2004)):

Equilibrium point: For the ordinary differential equation $\dot{X} = F(X)$, $X^* \in \mathbb{R}^n$ is an equilibrium point if $F(X^*) = 0$ for all t.

Asymptotically stable: Suppose $X^* \in \mathbb{R}^n$ is an equilibrium point for the differential equation, $\dot{X} = F(X)$. The X^* is a stable equilibrium if for every neighborhood $\mathcal{O}$ of X^* in $\mathbb{R}^n$ there is a neighborhood $\mathcal{O}_1$ of X^* in $\mathcal{O}$ such that every solution $X(t)$ with $X(0) = X_0$ in $\mathcal{O}_1$ is defined and remains in $\mathcal{O}$ for all $t > 0$. If $\mathcal{O}_1$ can be chosen so that, in addition to the properties for stability, we have $\lim_{t\to\infty} X(t) = X^*$, then we say that X^* is asymptotically stable. A sink is asymptotically stable and therefore stable, sources and saddles are examples of unstable equilibria.

Sink: For a linear system $\dot{X} = AX, X \in \mathbb{R}^n$, the equilibrium point is sink if and only if all eigenvalues of transition matrix A have negative real part.

Stable Equilibrium Point

We continue to take the two-link network as an example. Most of the time, the two-link network has 8 subspaces in the state space, where each subspace corresponds

to specific transition equations shown in Table 3.1 describing the dynamics of two link densities, the transition matrix A and the corresponding eigenvalues of each subspace are shown in Table 3.1 as well. By considering the influence of changing parameters, d_0, s_3, C_1, C_2, some subspaces are replaced by others, and the supplement information is shown in Table 3.2, Table 3.3.

According to Table 3.1, we can find that only the first three subspaces have sinks (stable equilibrium point), because all eigenvalues of the transition matrices of first three subspaces are negative. Then using the definition of the equilibrium point, we can get the expressions of the equilibrium point of different subspaces shown in Table 3.4.

As analyzed in section 3.2.2, with the increases of d_0, subspace 1 will transform to 1' when $d_0 > C_1$, at the meantime, the transformation of expressions of equilibrium point is shown in the first row of Table 3.4. Subspace 2 always exists in the state space as long as $d_0 > 0$. When C_2 reaches C_1 and continues to increase, subspace 3 will transform to 3", the variation of expressions of equilibrium point is shown in the third row of Table 3.4.

By taking the boundaries of subspaces into account, we only focus on stable equilibrium points within corresponding subspaces, the condition of occurrence is shown as follows:

Condition of the equilibrium point within the subspace 1: $d_0 \leq \min\{C_1, C_2, s_3\}$

Condition of the equilibrium point within the subspace 1': $C_1 \leq \min\{C_2, s_3, d_0\}$

Condition of the equilibrium point within the subspace 2: $s_3 \leq \min\{C_1, C_2, d_0\}$

Condition of the equilibrium point within the subspace 3: $C_2 \leq \min\{C_1, s_3, d_0\}$

Condition of the equilibrium point within the subspace 3": $C_2 \leq \min\{s_3, d_0\} \cap C_2 > C_1$.

Table 3.4: Equilibrium points of subspaces

Index	Sink	Index	Sink
1	$k_1 = \frac{d_0}{v_1}, k_2 = \frac{d_0}{v_2}$	1'	$k_1 = \frac{C_1}{v_1}, k_2 = \frac{C_1}{v_2}$

2	$k_1 = \frac{(\frac{w_1}{v_1}+1)C_1 - s_3}{w_1}$ $k_2 = \frac{(\frac{w_2}{v_2}+1)C_2 - s_3}{w_2}$		
3	$k_1 = \frac{(\frac{w_1}{v_1}+1)C_1 - C_2}{w_1}$ $k_2 = \frac{C_2}{v_2}$	3"	$k_1 = \frac{C_1}{v_1}, k_2 = \frac{C_1}{v_2}$

3.3 Observability

3.3.1 Concept of Observability

The concept of controllability and observability are proposed by Kalman (1960), which are dual to each other for a given state equation. Controllability studies steering the system states by inputs, on the contrary, observability studies determining the system states from outputs (observations). In this paper, we only focus on system observability, and assume that we have already known the transition equation.

Consider a general form of n-dimensional, p-input, q-output time-invariant linear system:

$$\dot{\boldsymbol{x}} = A\boldsymbol{x} + B\boldsymbol{u}, \tag{3.10a}$$

$$\boldsymbol{y} = C\boldsymbol{x} \tag{3.10b}$$

Where $\boldsymbol{x} \in \mathbb{R}^n$, $\boldsymbol{u} \in \mathbb{R}^p$, $\boldsymbol{y} \in \mathbb{R}^q$ are state variables, inputs, and outputs respectively, $A \in \mathbb{R}^{n\times n}$, $B \in \mathbb{R}^{n\times p}$, and $C \in \mathbb{R}^{q\times n}$ are constant matrices.

Definition (Chen (1999)): The state equation is said to be observable if for any unknown initial state $\boldsymbol{x}(0)$, there exists a finite $t_1 > 0$ such that the knowledge of the input u and the output $\boldsymbol{y}$ over $t \in [0, t_1]$ suffices to determine uniquely the initial state $\boldsymbol{x}(0)$. Otherwise, the equation is said to be unobservable.

3.3.2 Full Rank Test

Theorem **1**(Chen (1999)): The system (3.10) is observable if and one if the observability matrix O defined as (3.12) has full column rank.

Proof: By taking the derivatives of the continuous time measurements (3.10b), we can obtain:

$$
\begin{aligned}
&\boldsymbol{y}(0) = C\boldsymbol{x}(0)\\
&\dot{\boldsymbol{y}}(0) = C\dot{\boldsymbol{x}}(0) = CA\boldsymbol{x}(0) + C\boldsymbol{u}(0)\\
&\ddot{\boldsymbol{y}}(0) = C\ddot{\boldsymbol{x}}(0) = CA^2\boldsymbol{x}(0) + CA\boldsymbol{u}(0) + C\dot{\boldsymbol{u}}(0)\\
&\vdots\\
&\boldsymbol{y}^{(n-1)}(0) = C\boldsymbol{x}^{(n-1)}(0) = CA^{n-1}\boldsymbol{x}(0) + CA^{n-2}\boldsymbol{u}(0) + \cdots + C\boldsymbol{u}^{(n-2)}(0)
\end{aligned}
$$

Above equations consists of nq linear equations, which could be transformed in matrix form as:

$$
\begin{bmatrix} \boldsymbol{y}(0) \\ \dot{\boldsymbol{y}}(0) \\ \ddot{\boldsymbol{y}}(0) \\ \vdots \\ \boldsymbol{y}^{(n-1)}(0) \end{bmatrix}^{(nq)\times 1} = \begin{bmatrix} C \\ CA \\ CA^2 \\ \vdots \\ CA^{n-1} \end{bmatrix}^{(nq)\times n} \times \boldsymbol{x}(0) + D \begin{bmatrix} \boldsymbol{u}(0) \\ \dot{\boldsymbol{u}}(0) \\ \ddot{\boldsymbol{u}}(0) \\ \vdots \\ \boldsymbol{u}^{(n-2)}(0) \end{bmatrix}^{p(n-1)\times 1} \tag{3.11}
$$

where $D = \begin{bmatrix} 0 & 0 & 0 & \dots & 0 \\ CB & 0 & 0 & \dots & 0 \\ CAB & CB & 0 & \dots & 0 \\ \vdots & \vdots & & & \vdots \\ CA^{n-2}B & CA^{n-3}B & CA^{n-4}B & \dots & CB \end{bmatrix}^{(nq)\times p(n-1)}$.

We define the observability matrix O as below:

$$O = \begin{bmatrix} C \\ CA \\ CA^2 \\ \vdots \\ CA^{n-1} \end{bmatrix} \tag{3.12}$$

Because the output, input, matrix A and B are known, the initial condition $x(0)$ can be determined uniquely from (3.11) if and only if the observability matrix O has full column rank, rank(O)=n.

Example: Consider a linear dynamical system with:

$$A = \begin{bmatrix} -1 & 0 & 0 \\ 0 & -2 & 0 \\ 1 & 2 & -3 \end{bmatrix}, C = \begin{bmatrix} 0 & 0 & 1 \end{bmatrix}$$

We can calculate the observabiltiy matrix O as:

$$O = \begin{bmatrix} 0 & 0 & 1 \\ 1 & 2 & -3 \\ -4 & -10 & 9 \end{bmatrix}$$

Which is nonsingular with rank(O)=3, the system is observable.

3.3.3 PBH Test

***Theorem* 2**: The system (A, C) is observable if and only if there exists no non-zero vector $\boldsymbol{p} \in \mathbb{R}^n$ such that:

$$A\boldsymbol{p} = \lambda\boldsymbol{p}, C\boldsymbol{p} = \mathbf{0} \tag{3.13}$$

***Proof* :** The theorem 2 could be proved if the following statement is true:

The system (A, C) is unobservable if and only if there exists a non-zero vector $\boldsymbol{p} \in \mathbb{R}^n$ such that $A\boldsymbol{p} = \lambda\boldsymbol{p}$ and $C\boldsymbol{p} = \mathbf{0}$ for some $\lambda \neq 0$.

Firstly, we assume there exists a non-zero vector $\boldsymbol{p} \in \mathbb{R}^n$, which satisfies the conditions, and multiplies it by observability matrix O:

$$O\boldsymbol{p} = \begin{bmatrix} C \\ CA \\ CA^2 \\ \vdots \\ CA^{n-1} \end{bmatrix} \boldsymbol{p} = \begin{bmatrix} C\boldsymbol{p} \\ \lambda C\boldsymbol{p} \\ \lambda^2 C\boldsymbol{p} \\ \vdots \\ \lambda^{n-1} C\boldsymbol{p} \end{bmatrix} = \mathbf{0}$$

Thus, observability matrix O is singular and the system (A, C) is unobservable.

Now we assume that the system (A, C) is unobservable, based on Kalman canonical decomposition, the system could be separated into observable and unobservable parts by a transformation matrix T like:

$$\hat{A} = \begin{bmatrix} \hat{A}_o & \mathbf{0} \\ \hat{A}_{21} & \hat{A}_u \end{bmatrix}, \hat{C} = \begin{bmatrix} \hat{C}_o & \mathbf{0} \end{bmatrix}$$

Then, for any eigenvector $\boldsymbol{p}_u$ of $\hat{A}^u$, we could obtain $\boldsymbol{p}^T = [\mathbf{0} \quad \boldsymbol{p}_u^T]$, which satisfies the following conditions:

$$\hat{A}\boldsymbol{p} = \lambda \boldsymbol{p}, \hat{C}\boldsymbol{p}$$

$$T^{-1}AT\boldsymbol{p} = \lambda \boldsymbol{p}, CT\boldsymbol{p} = \mathbf{0}$$

$$AT\boldsymbol{p} = \lambda T\boldsymbol{p}, CT\boldsymbol{p} = \mathbf{0}$$

Therefore, there exists a vector $T\boldsymbol{p}$, satisfies the condition of the theorem.

Theorem **3**: The system (A, C) is observable if and only if rank $\begin{bmatrix} sI - A \\ C \end{bmatrix} = n$, for all $s \in \mathbb{R}$.

Proof: If rank $\begin{bmatrix} sI - A \\ C \end{bmatrix} = n$, the nullspace of $\begin{bmatrix} sI - A \\ C \end{bmatrix}$ is empty, there not exists

a non-zero $\boldsymbol{p} \in \mathbb{R}^n$ such that:

$$\begin{bmatrix} sI - A \\ C \end{bmatrix} \boldsymbol{p} = \mathbf{0}, \forall s \in \mathbb{R} \tag{3.14}$$

Then by theorem 2, the system (A, C) is observable. The converse could be easily obtained by reversing the above proof.

Example: Consider a linear dynamical system with:

$$A = \begin{bmatrix} -1 & 0 & 0 \\ 0 & -1 & 0 \\ 1 & 1 & -3 \end{bmatrix}, C = \begin{bmatrix} 1 & 0 & 0 \\ 0 & 0 & 1 \end{bmatrix}$$

If $(sI - A)\boldsymbol{p} \neq \mathbf{0}$, equivalently, s is not one of the eigenvalues of A, there not exists a non-zero $\boldsymbol{p} \in \mathbb{R}^n$ such that $\begin{bmatrix} sI - A \\ C \end{bmatrix} \boldsymbol{p} = \mathbf{0}$, which is equal to rank $\begin{bmatrix} sI - A \\ C \end{bmatrix} = n$.
If $(sI - A)\boldsymbol{p} = \mathbf{0}$, equivalently, s is one of the eigenvalues of A. Matrix A has three eigenvalues, repeated $s_1 = s_2 = -1$ and distinct $s_3 = -3$.

Bring $s_1 = s_2 = -1$ into equation(3.14):

$$\text{rank} \begin{bmatrix} s_1 I - A \\ C \end{bmatrix} = rank \begin{bmatrix} 0 & 0 & 0 \\ 0 & 0 & 0 \\ -1 & -1 & 2 \\ 1 & 0 & 0 \\ 0 & 0 & 1 \end{bmatrix} = 3$$

Bring $s_3 = -3$ into equation(3.14):

$$\text{rank} \begin{bmatrix} s_3 I - A \\ C \end{bmatrix} = rank \begin{bmatrix} -2 & 0 & 0 \\ 0 & -2 & 0 \\ -1 & -1 & 0 \\ 1 & 0 & 0 \\ 0 & 0 & 1 \end{bmatrix} = 3$$

In a nutshell, rank $\begin{bmatrix} sI - A \\ C \end{bmatrix} = 3$ for all $s \in \mathbb{R}$, the system is observable.

Chapter 4

Numerical Examples

In this chapter, to begin with, given transition matrix A of stable subspaces of ordinary, merging, and diverging junctions, we will show the corresponding measurement matrix C, which guarantees the full observability. Then we will give two examples of small expressway networks and discuss the relationship among network topology, congestion conditions, and measurement matrix C for full observability.

4.1 Examples of Different Junctions

Any network could be partitioned into three types of junctions, ordinary, merging, and diverging, so we only focus on these three junctions in this section. Moreover, the number of subspaces will explode as the network becomes more and more complex, and stable subspaces, which contain stable equilibrium point under some conditions, are more critical than unstable ones. Therefore, we only display the measurement matrix C for stable subspaces of the three junctions.

Based on the full rank test or PBH test introduced in the last chapter and given transition matrix A of each stable subspace, we could obtain the corresponding measurement matrix C, which makes sure the system within that subspace is observable. The congestion condition, transition matrix A, and corresponding measurement matrix

C of each stable subspace are shown in Table 4.1 for ordinary junction, Table 4.2 for diverging junction, and Table 4.3 for merging junction, where F and C in congestion condition column denote light traffic, $k_a(t) \leq k_{a,c}$, and congestion, $k_a(t) > k_{a,c}$, of link respectively.

Clearly, there is no one-to-one or onto mapping between congestion conditions and subspaces, the total number of congestion conditions of n-link is 2^n, the total number of subspaces is much bigger. Mostly, a stable subspace is included in the range of a congestion condition, however, exception will occur when split ratio is equal to the ratio of supplies for diverge junction. We use congestion condition here to reflect the traffic condition of each stable subspace.

Table 4.1: Measurement matrix C of stable subspaces of ordinary junction

Congestion Condition	Transition Matrix A	Measurement Matrix C
$F - F$	$\begin{bmatrix} -v_1 & 0 \\ v_1 & -v_2 \end{bmatrix}$	$\begin{bmatrix} 0 & 1 \end{bmatrix}$
$C - C$	$\begin{bmatrix} -w_1 & w_2 \\ 0 & -w_2 \end{bmatrix}$	$\begin{bmatrix} 1 & 0 \end{bmatrix}$
$C - F$	$\begin{bmatrix} -w_1 & 0 \\ 0 & -v_2 \end{bmatrix}$	$\begin{bmatrix} 1 & 0 \\ 0 & 1 \end{bmatrix}$

According to Table 4.1, we can find there are three congestion conditions for stable subspaces of the 2-link ordinary junction. Also, we need to observe the last link of successive light traffic links and the first link of successive congested links to achieve system full observability.

Table 4.2: Measurement matrix C of stable subspaces of diverge junction

Congestion Condition	Transition Matrix A	Measurement Matrix C
$F-\begin{matrix}F\\F\end{matrix}$	$\begin{bmatrix} -v_1 & 0 & 0 \\ \xi_{12}v_1 & -v_2 & 0 \\ \xi_{13}v_1 & 0 & -v_3 \end{bmatrix}$	$\begin{bmatrix} 0 & 1 & 0 \\ 0 & 0 & 1 \end{bmatrix}$
$C-\begin{matrix}F\\F\end{matrix}$	$\begin{bmatrix} -w_1 & 0 & 0 \\ 0 & -v_2 & 0 \\ 0 & 0 & -v_3 \end{bmatrix}$	$\begin{bmatrix} 1 & 0 & 0 \\ 0 & 1 & 0 \\ 0 & 0 & 1 \end{bmatrix}$
$C-\begin{matrix}C\\F\end{matrix}$	$\begin{bmatrix} -w_1 & \frac{w_2}{\xi_{12}} & 0 \\ 0 & -w_2 & 0 \\ 0 & \frac{-w_2\xi_{13}}{\xi_{12}} & -v_3 \end{bmatrix}$	$\begin{bmatrix} 1 & 0 & 0 \\ 0 & 0 & 1 \end{bmatrix}$
$C-\begin{matrix}F\\C\end{matrix}$	$\begin{bmatrix} -w_1 & 0 & \frac{w_3}{\xi_{13}} \\ 0 & -v_2 & \frac{-w_3\xi_{12}}{\xi_{13}} \\ 0 & 0 & -w_3 \end{bmatrix}$	$\begin{bmatrix} 1 & 0 & 0 \\ 0 & 1 & 0 \end{bmatrix}$
$C-\begin{matrix}C\\C\end{matrix}$ or $C-\begin{matrix}C\\F\end{matrix}$	$\begin{bmatrix} -w_1 & \frac{w_2}{\xi_{12}} & 0 \\ 0 & -w_2 & 0 \\ 0 & \frac{-w_2\xi_{13}}{\xi_{12}} & 0 \end{bmatrix}$	$\begin{bmatrix} 1 & 0 & 0 \\ 0 & 0 & 1 \end{bmatrix}$
$C-\begin{matrix}C\\C\end{matrix}$ or $C-\begin{matrix}F\\C\end{matrix}$	$\begin{bmatrix} -w_1 & 0 & \frac{w_3}{\xi_{13}} \\ 0 & 0 & \frac{-w_3\xi_{12}}{\xi_{13}} \\ 0 & 0 & -w_3 \end{bmatrix}$	$\begin{bmatrix} 1 & 0 & 0 \\ 0 & 1 & 0 \end{bmatrix}$

According to Table 4.2, besides the same rule of full observability mentioned ahead, we find stable equilibrium points also appear in subspaces with rank 2, like the last two rows. If the ratio of split ratio is equal to the ratio of supplies, $\frac{\xi_{12}}{\xi_{13}} = \frac{s_4}{s_5}$, the trajectories with any initial condition will end at subspaces with rank 2. Otherwise, the trajectories with any initial condition will end at subspaces with full rank, like two

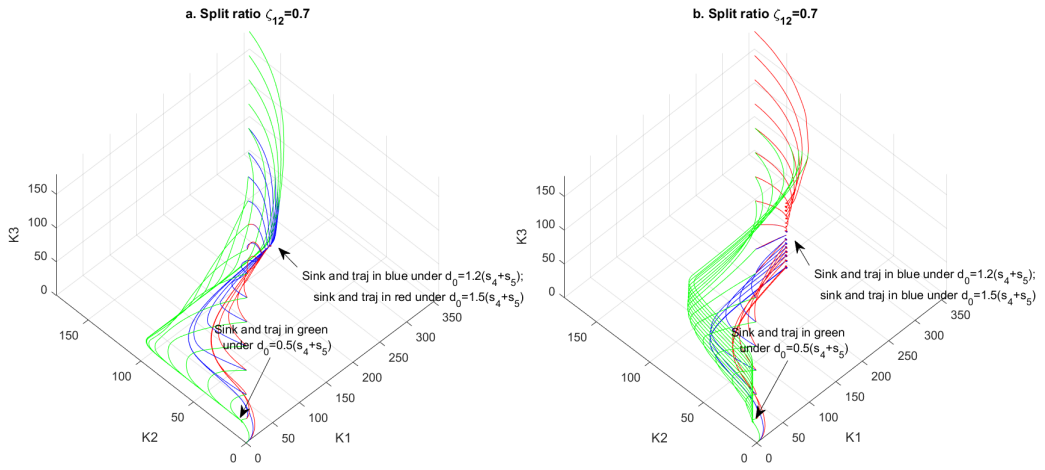

Figure 4.1: Trajectories and stable equilibrium point of two examples

rows in the middle. Two examples of trajectories with different initial conditions and stable equilibrium points are shown in Figure 4.1. Figure 4.1a shows that when link capacities are 4680 veh/h, 2340 veh/h, 2340 veh/h respectively, split ratios are $\xi_{12} = 0.7$ and $\xi_{13} = 0.3$, supplies are $s_4 = 1170veh/h$ and $s_5 = 1170veh/h$, trajectories in green with condition $d_0 = 0.5(s_4 + s_5)$ end at one of the subspaces whose transition matrix A is shown in the first row of Table 4.2, trajectories in blue with condition $d_0 = 1.2(s_4+s_5)$ and those in red with condition $d_0 = 1.5(s_4 + s_5)$ end at one of the subspaces whose transition matrix is shown in the third row of Table 4.2. Figure 4.1b shows that when link capacities are 4680 veh/h, 2340 veh/h, 2340 veh/h respectively, split ratios are $\xi_{12} = 0.7$ and $\xi_{13} = 0.3$, supplies are $s_4 = 0.7 \times 2340veh/h$ and $s_5 = 0.3 \times 2340veh/h$, trajectories in green with condition $d_0 = 0.5(s_4 + s_5)$ end at one of the subspaces whose transition matrix A is shown in the first row of Table 4.2, trajectories in blue with condition $d_0 = 1.2(s_4 + s_5)$ and those in red with condition $d_0 = 1.5(s_4 + s_5)$ end at one of the subspaces whose transition matrix is shown in the fifth row of Table 4.2, and still in these subspaces, the congestion condition of link 3 is uncertain.

Table 4.3: Measurement matrix C of stable subspaces of Merge junction

Congestion Condition	Transition Matrix A	Measurement Matrix C

$\begin{matrix} F \\ F \end{matrix} - F$	$\begin{bmatrix} -v_1 & 0 & 0 \\ 0 & -v_2 & 0 \\ v_1 & v_2 & -v_3 \end{bmatrix}$	$if v_1 \neq v_2, \begin{bmatrix} 0 & 0 & 1 \end{bmatrix}$ $if v_1 = v_2, \begin{bmatrix} 1 & 0 & 0 \\ 0 & 0 & 1 \end{bmatrix}$ $or \begin{bmatrix} 0 & 1 & 0 \\ 0 & 0 & 1 \end{bmatrix}$
$\begin{matrix} C \\ F \end{matrix} - F$	$\begin{bmatrix} -w_1 & 0 & 0 \\ 0 & -v_2 & 0 \\ 0 & v_2 & -v_3 \end{bmatrix}$	$\begin{bmatrix} 1 & 0 & 0 \\ 0 & 0 & 1 \end{bmatrix}$
$\begin{matrix} F \\ C \end{matrix} - F$	$\begin{bmatrix} -v_1 & 0 & 0 \\ 0 & -w_2 & 0 \\ v_1 & 0 & -v_3 \end{bmatrix}$	$\begin{bmatrix} 0 & 1 & 0 \\ 0 & 0 & 1 \end{bmatrix}$
$\begin{matrix} C \\ C \end{matrix} - F$	$\begin{bmatrix} -w_1 & 0 & 0 \\ 0 & -w_2 & 0 \\ 0 & 0 & -v_3 \end{bmatrix}$	$\begin{bmatrix} 1 & 0 & 0 \\ 0 & 1 & 0 \\ 0 & 0 & 1 \end{bmatrix}$
$\begin{matrix} C \\ F \end{matrix} - C$	$\begin{bmatrix} -w_1 & v_2 & w_3 \\ 0 & -v_2 & 0 \\ 0 & 0 & -w_3 \end{bmatrix}$	$\begin{bmatrix} 1 & 0 & 0 \end{bmatrix}$
$\begin{matrix} F \\ C \end{matrix} - C$	$\begin{bmatrix} -v_1 & 0 & 0 \\ v_1 & -w_2 & w_3 \\ 0 & 0 & -w_3 \end{bmatrix}$	$\begin{bmatrix} 0 & 1 & 0 \end{bmatrix}$
$\begin{matrix} C \\ C \end{matrix} - C$	$\begin{bmatrix} -w_1 & 0 & \frac{C_1 w_3}{C_1+C_2} \\ 0 & -w_2 & \frac{C_2 w_3}{C_1+C_2} \\ 0 & 0 & -w_3 \end{bmatrix}$	$\begin{bmatrix} 1 & 0 & 0 \\ 0 & 1 & 0 \end{bmatrix}$

According to Table 4.3, we can find that the rule of full observability concluded based on the former cases is violated. In the fifth and the sixth row, because the

dynamics of link 1 density and link 2 density include all link information, we only need to observe link 1 in subspaces whose transition matrix is shown in the second row and link 2 in subspaces whose transition matrix is shown in the third row. In addition, if the symmetry happens, that is link 1 and link 2 share the same free flow speed, like the example shown in the first row, besides observing link 3, which contains all link information, we still need to observe one of the first two links to distinguish them.

4.1.1 Example of 5-link Corridor Without Ramps

Firstly, we consider a simpler case, a 5-link corridor without ramps, which consists of ordinary junctions only. The network topology is shown in Figure 4.2. The network congestion condition, transition matrix, and corresponding measurement matrix for full observability of each stable subspace are shown in Table 4.4.

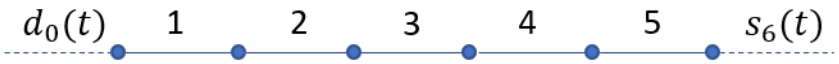

Figure 4.2: Corridor without ramps

Table 4.4: Measurement matrix C of stable subspaces of corridor without ramps

Congestion Condition	Transition Matrix A	Measurement Matrix C
$FFFFF$	$\begin{bmatrix} -v_1 & 0 & 0 & 0 & 0 \\ v_1 & -v_2 & 0 & 0 & 0 \\ 0 & v_2 & -v_3 & 0 & 0 \\ 0 & 0 & v_3 & -v_4 & 0 \\ 0 & 0 & 0 & v_4 & -v_5 \end{bmatrix}$	$\begin{bmatrix} 0 & 0 & 0 & 0 & 1 \end{bmatrix}$

$CFFFF$	$\begin{bmatrix} -w_1 & 0 & 0 & 0 & 0 \\ 0 & -v_2 & 0 & 0 & 0 \\ 0 & v_2 & -v_3 & 0 & 0 \\ 0 & 0 & v_3 & -v_4 & 0 \\ 0 & 0 & 0 & v_4 & -v_5 \end{bmatrix}$	$\begin{bmatrix} 1 & 0 & 0 & 0 & 0 \\ 0 & 0 & 0 & 0 & 1 \end{bmatrix}$
$CCFFF$	$\begin{bmatrix} -w_1 & w_2 & 0 & 0 & 0 \\ 0 & -w_2 & 0 & 0 & 0 \\ 0 & 0 & -v_3 & 0 & 0 \\ 0 & 0 & v_3 & -v_4 & 0 \\ 0 & 0 & 0 & v_4 & -v_5 \end{bmatrix}$	$\begin{bmatrix} 1 & 0 & 0 & 0 & 0 \\ 0 & 0 & 0 & 0 & 1 \end{bmatrix}$
$CCCFF$	$\begin{bmatrix} -w_1 & w_2 & 0 & 0 & 0 \\ 0 & -w_2 & w_3 & 0 & 0 \\ 0 & 0 & -w_3 & 0 & 0 \\ 0 & 0 & 0 & -v_4 & 0 \\ 0 & 0 & 0 & v_4 & -v_5 \end{bmatrix}$	$\begin{bmatrix} 1 & 0 & 0 & 0 & 0 \\ 0 & 0 & 0 & 0 & 1 \end{bmatrix}$
$CCCCF$	$\begin{bmatrix} -w_1 & w_2 & 0 & 0 & 0 \\ 0 & -w_2 & w_3 & 0 & 0 \\ 0 & 0 & -w_3 & w_4 & 0 \\ 0 & 0 & 0 & -w_4 & 0 \\ 0 & 0 & 0 & 0 & -v_5 \end{bmatrix}$	$\begin{bmatrix} 1 & 0 & 0 & 0 & 0 \\ 0 & 0 & 0 & 0 & 1 \end{bmatrix}$
$CCCCC$	$\begin{bmatrix} -w_1 & w_2 & 0 & 0 & 0 \\ 0 & -w_2 & w_3 & 0 & 0 \\ 0 & 0 & -w_3 & w_4 & 0 \\ 0 & 0 & 0 & -w_4 & w_5 \\ 0 & 0 & 0 & 0 & -w_5 \end{bmatrix}$	$\begin{bmatrix} 1 & 0 & 0 & 0 & 0 \end{bmatrix}$

From Table 4.4, there are 6 stable network states of the 5-link corridor without ramps. When a queue starts to form, the shock wave will propagate backward, so the congestion state always continues to the first upstream link. Expect for the first and the last row, congestion conditions in other rows exists a shift from congestion to light traffic state. This is because the outflux of the link where the queue begins to form equals the minimum capacity of this link and the adjacent downstream link, in other words, the shift will happen when a queue accumulates in the link, and the adjacent downstream link has enough spare space.

4.1.2 Example of Corridor with On- and Off- ramps

Now, we will take on- and off-ramp into consideration, the structure of a network consisting of a merging junction and a diverging junction is shown in Figure 4.3. According to the network topology, the merging junction and the diverging junction share the link 3. Intuitively, this network's stable network congestion conditions are the combination of merging and diverging junctions under the restriction that the congestion status of the shared link is consistent. For instance, if the last link of the diverging junction is congested, the first link of the diverging junction will be congested as well.

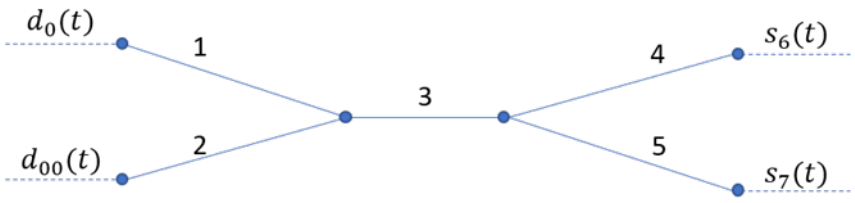

Figure 4.3: Corridor with ramps

We can obtain the corresponding transition matrix with the known congestion status of the network and then search the measurement matrix C by utilizing the full rank test or PBH test. In addition, we find that if the shared link needs to be observed in the merging junction and its information could be inferred by other links in the diverging junction, we need not to observe it anymore for the full observability.

Examples are shown in Table 4.5.

Table 4.5: Measurement matrix C of stable subspaces of corridor without ramps

Congestion Condition	Transition Matrix A	Measurement Matrix C
$\begin{matrix} F & & F \\ & F & \\ F & & F \end{matrix}$	$\begin{bmatrix} -v_1 & 0 & 0 & 0 & 0 \\ 0 & -v_2 & 0 & 0 & 0 \\ v_1 & v_2 & -v_3 & 0 & 0 \\ 0 & 0 & \xi_{34}v_3 & -v_4 & 0 \\ 0 & 0 & \xi_{35}v_3 & v_4 & -v_5 \end{bmatrix}$	$if v_1 \neq v_2, \begin{bmatrix} 0 & 0 & 0 & 1 & 0 \\ 0 & 0 & 0 & 0 & 1 \end{bmatrix}$ $if v_1 = v_2, \begin{bmatrix} 1 & 0 & 0 & 0 & 0 \\ 0 & 0 & 0 & 1 & 0 \\ 0 & 0 & 0 & 0 & 1 \end{bmatrix}$ $or \begin{bmatrix} 0 & 1 & 0 & 0 & 0 \\ 0 & 0 & 0 & 1 & 0 \\ 0 & 0 & 0 & 0 & 1 \end{bmatrix}$
$\begin{matrix} C & & F \\ & F & \\ C & & F \end{matrix}$	$\begin{bmatrix} -w_1 & 0 & 0 & 0 & 0 \\ 0 & -w_2 & 0 & 0 & 0 \\ 0 & 0 & -v_3 & 0 & 0 \\ 0 & 0 & \xi_{34}v_3 & -v_4 & 0 \\ 0 & 0 & \xi_{35}v_3 & v_4 & -v_5 \end{bmatrix}$	$\begin{bmatrix} 1 & 0 & 0 & 0 & 0 \\ 0 & 1 & 0 & 0 & 0 \\ 0 & 0 & 0 & 1 & 0 \\ 0 & 0 & 0 & 0 & 1 \end{bmatrix}$

In a nutshell, under stable conditions, we could decompose the network into three types of junctions and then determine which links need to be observed to achieve network full observability based on Table 4.1, 4.2, 4.3 with considering shockwave propagation. Generally, we need to observe the last link of the successive light traffic links and the first one of the successive congested links to achieve full observability. However, there exist some exceptions like symmetry merge, which will appear when the infrastructure conditions of the merge links are the same, and we need to add sensors to distinguish merge links. The exception shows the relationship between the measurement matrix and eigenvalues of a certain transition matrix. In addition to the

position of the transition matrix elements, the values of the transition matrix elements will also affect the final determination of the measurement matrix. For unstable conditions of the system, the number of congestion condition will explode when the network topology becomes more and more complex, the above observations will be violated. Therefore, we are going to explore the relationship between eigenvalues, eigenvectors, and measurement matrix, and expect to find a more general approach to determine which links need to be observed for the system full observability in the future.

Chapter 5

Conclusions and Discussion

5.1 Conclusion

The thesis analyzed the observability problem in the dynamic system setting. Compared with studies in the static setting, in which the relationship between link densities is only described by network topology, this model also considers the traffic operational and temporal relations to infer link densities that cannot be observed directly.

In virtue of the link queue model based on a triangular fundamental diagram to describe traffic dynamics, the nonlinear traffic system could be approximated by a switched linear system by separating the state space into subspaces in which the system is time-invariant linear. Therefore, we could extend the observability analysis from the equilibrium point to stable subspaces even to the whole space.

In particular, properties of the link queue model including phase transition, boundary variation, and stability are analyzed, which could help us understand traffic network dynamics better. We found that each subspace corresponds to a specific network traffic state in reality. Any trajectory of the solution of our piecewise affine system will move across a lot of subspaces and end at the equilibrium point, this process is in accord with shock wave or rarefaction wave propagation on links. There exists only one equi-

librium point in the whole space and it will transfer to different subspaces according to the changes in parameters. In addition, from experiments on the boundary variation with parameters, we found that some subspace will disappear for a certain range of parameters, but the subspace with equilibrium point always exists. So we determined the equilibrium point and the boundaries of subspaces containing the equilibrium point and set them as objectives to conduct observability analysis.

In observability analysis, the full rank test and PBH test are employed as conditions for searching the measurement matrix of full observability by enumeration. Besides the corridor network without ramps, we considered merge and diverge junctions to improve the network complexity. According to our examples, generally, the last link of successive light traffic links and the first one of successive congested links need to be observed to achieve full observability. However, there exist some exceptions, like symmetry merge, which appears when the transition matrix has repeated eigenvalues, and on behalf of the same infrastructure condition of merge links in reality, so we need to add more sensors to distinguish merge links. This exception also shows that in addition to the relationship between positions of transition matrix elements and measurement matrix, the exact value of transition matrix elements matters as well.

5.2 Limitaions

The main limitations of this study are listed below:

(a) As the network becomes more and more complicated, the number of subspaces will explode, and the subspaces within the studied state space are changing continuously as the parameters change. So, it is too difficult to analyze system properties, including observability and stability, for all subspaces.

(b) In this thesis, the demands and supplies of the network are constants. The network could always end at an equilibrium point and reach a stable state. However, the demands and supplies are changing with time in reality, the trajectory of the solution

of our piecewise affine system will move across different series of subspaces, the static sensor deployment strategy described in this thesis is not enough, a dynamic sensor deployment strategy is needed.

(c) We assume the split ratio is known for any diverging junction, which is hard to measure based on counting sensors in real life.

5.3 Future Works

(a) Currently, our network traffic flow model is deterministic, we could add stochastic elements in the initial condition, the boundary flow, and the fundamental diagram to extend it into a stochastic model, which might describe the traffic dynamics more accurately.

(b) Method of solving the subspace explosion is expected. For example, the transition matrix that describes the traffic dynamics could be transformed from the time-invariant of each subspace into a general form. Each entry of the transition matrix could be expressed by a function of parameters, like demands, supplies, and link capacities.

(c) According to examples shown in chapter 4, there is a big difference among observations for full observability under different network congestion conditions. If we want to obtain full observability under any network condition, we maybe need to observe all links. If we use counting sensors only, equipping all links with sensors is unpractical. We could propose an optimization problem by setting the objective to gain the most link information and cost the least in future studies. If we also consider mobile sensors, we need to know the optimal location of counting sensors and the arrangement of mobile sensors.

(d) As the number of links increases, the computation work of searching measurement matrix by enumeration surges, we expect to find a more systematic approach to determine the measurement matrix by considering the relationship between eigenvalues, eigenvectors, and measurement matrix.

(e) Sensor error could also be considered to improve the accuracy of direct observations and indirect deductions of links.

References

Agarwal, S., Kachroo, P., Contreras, S., 2016. A Dynamic Network Modeling-Based Approach for Traffic Observability Problem. IEEE Transactions on Intelligent Transportation Systems 17, 1168–1178. doi:10.1109/TITS.2015.2499538.

Boel, R., Mihaylova, L., 2006. A compositional stochastic model for real time freeway traffic simulation. Transportation Research Part B: Methodological 40, 319–334. doi:10.1016/j.trb.2005.05.001.

Carey, M., McCartney, M., 2004. An exit-flow model used in dynamic traffic assignment. Computers and Operations Research 31, 1583–1602. doi:10.1016/S0305-0548(03)00109-6.

Castillo, E., Calvino, A., Menendez, J.M., Jimenez, P., Rivas, A., 2013. Deriving the upper bound of the number of sensors required to know all link flows in a traffic network. IEEE Transactions on Intelligent Transportation Systems 14, 761–771. doi:10.1109/TITS.2012.2233474.

Castillo, E., Conejo, A.J., Menéndez, J.M., Jiménez, P., 2008. The observability problem in traffic network models. Computer-Aided Civil and Infrastructure Engineering 23, 208–222. doi:10.1111/j.1467-8667.2008.00531.x.

Castillo, E., Grande, Z., Calviño, A., Szeto, W.Y., Lo, H.K., 2015. A State-of-The-Art Review of the Sensor Location, Flow Observability, Estimation, and Prediction Problems in Traffic Networks. Journal of Sensors 2015. doi:10.1155/2015/903563.

Castillo, E., Rivas, A., Jiménez, P., Menéndez, J.M., 2012. Observability in traffic networks. Plate scanning added by counting information. Transportation 39, 1301–1333. doi:10.1007/s11116-012-9390-0.

Chen, C.T., 1999. Linear system theory and design. Oxford series in electrical and computer engineering. 3rd ed. ed., Oxford University Press, New York.

Daganzo, C.F., 1992. The cell transmission model, part I: A simple dynamic representation of highway traffic. Technical Report. Institute of Transportation Studies.

Daganzo, C.F., 1995. The cell transmission model, part II: Network traffic. Transportation Research Part B: Methodological 29, 79–93. doi:10.1016/0191-2615(94)00022-R.

Daganzo, C.F., 1999. The lagged cell-transmission model, in: Proceedings of the fourteenth International Symposium on Transportation and Traffic Theory, pp. 147–171. URL: http://citeseerx.ist.psu.edu/viewdoc/summary?doi=10.1.1.40.8310.

Gentili, M., Mirchandani, P.B., 2012. Locating sensors on traffic networks: Models, challenges and research opportunities. Transportation Research Part C: Emerging Technologies 24, 227–255. URL: http://dx.doi.org/10.1016/j.trc.2012.01.004, doi:10.1016/j.trc.2012.01.004.

Gipps, P.G., 1986. A model for the structure of lane-changing decisions. Transportation Research Part B 20, 403–414. doi:10.1016/0191-2615(86)90012-3.

He, S.X., 2013. A graphical approach to identify sensor locations for link flow inference. Transportation Research Part B: Methodological 51, 65–76. URL: http://dx.doi.org/10.1016/j.trb.2013.02.006, doi:10.1016/j.trb.2013.02.006.

Hirsch, M.W., 2004. Differential equations, dynamical systems, and an introduction

to chaos. Pure and applied mathematics (Academic Press) ; 60. 2nd ed. ed., Elsevier/Academic Press, Amsterdam ; Boston.

Hu, S.R., Peeta, S., Chu, C.H., 2009. Identification of vehicle sensor locations for link-based network traffic applications. Transportation Research Part B: Methodological 43, 873–894. URL: http://dx.doi.org/10.1016/j.trb.2009.02.008, doi:10.1016/j.trb.2009.02.008.

Jabari, S.E., Liu, H.X., 2012. A stochastic model of traffic flow: Theoretical foundations. Transportation Research Part B: Methodological 46, 156–174. doi:10.1016/j.trb.2011.09.006.

Jin, W.L., 2017. A Riemann solver for a system of hyperbolic conservation laws at a general road junction. Transportation Research Part B: Methodological 98, 21–41. doi:10.1016/j.trb.2016.12.007, arXiv:1204.6727.

Jin, W.L., 2021. A link queue model of network traffic flow. Transportation Science 55, 436–455. doi:10.1287/TRSC.2020.1012, arXiv:1209.2361.

Kalman, R., 1960. On the general theory of control systems, in: IFAC Proceedings Volumes, Elsevier. pp. 491–502. URL: http://dx.doi.org/10.1016/S1474-6670(17)70094-8, doi:10.1016/s1474-6670(17)70094-8.

Lighthill, M.J., Whitham, G.B., 1955a. On Kinematic Waves . II . A Theory of Traffic Flow on Long Crowded Roads. Proceedings of the Royal Society of London. Series A. Mathematical and Physical Sciences 229, 317–345.

Lighthill, M.J., Whitham, G.B., 1955b. On kinematic waves I. Flood movement in long rivers. Proceedings of the Royal Society of London. Series A. Mathematical and Physical Sciences 229, 281–316. doi:10.1098/rspa.1955.0088.

Liu, Y.Y., Slotine, J.J., Barabasi, A.L., 2013. Observability of complex systems. Proceedings of the National Academy of Sciences of the United States of America 110, 2460–2465. doi:10.1073/pnas.1215508110.

Merchant, D.K., Nemhauser, G.L., 1978. A Model and an Algorithm for the Dynamic Traffic Assignment Problems. Transportation Science 12, 183–199. doi:10.1016/S0191-2615(97)00026-X.

Mori, H., Tsuzuki, S., 1991. A Fast Method for Topological Observability Analysis Using a Minimum Spanning Tree Technique. IEEE Transactions on Power Systems 6, 491–500. doi:10.1109/59.76691.

Muñoz, L., Sun, X., Horowitz, R., Alvarez, L., 2003. Traffic Density Estimation with the Cell Transmission Model. Proceedings of the American Control Conference 5, 3750–3755. doi:10.1109/acc.2003.1240418.

Newell, G.F., 1993. A simplified theory of kinematic waves in highway traffic, part I: General theory. Transportation Research Part B 27, 281–287. doi:10.1016/0191-2615(93)90039-D.

Newell, G.F., 2002. A simplified car-following theory: A lower order model. Transportation Research Part B: Methodological 36, 195–205. doi:10.1016/S0191-2615(00)00044-8.

Ng, M.W., 2012. Synergistic sensor location for link flow inference without path enumeration: A node-based approach. Transportation Research Part B: Methodological 46, 781–788. URL: http://dx.doi.org/10.1016/j.trb.2012.02.001, doi:10.1016/j.trb.2012.02.001.

Papageorgiou, M., Blosseville, J.M., Hadj-Salem, H., 1990. Modelling and real-time control of traffic flow on the southern part of Boulevard Peripherique in Paris: Part

I: Modelling. Transportation Research Part A: General 24, 345–359. doi:10.1016/0191-2607(90)90047-A.

Prigogine, I., Andrews, F.C., 1960. A Boltzmann-Like Approach for Traffic Flow. Operations Research 8, 789–797.

Richards, P.I., 1956. Shock Waves on the Highway. Operations Research 4, 42–51.

Rostami-Shahrbabaki, M., Safavi, A.A., Papageorgiou, M., Setoodeh, P., Papamichail, I., 2020. State estimation in urban traffic networks: A two-layer approach. Transportation Research Part C: Emerging Technologies 115, 102616. URL: https://doi.org/10.1016/j.trc.2020.102616, doi:10.1016/j.trc.2020.102616.

Schreckenberg, M., Schadschneider, A., Nagel, K., Ito, N., 1995. Discrete stochastic models for traffic flow. Physical Review E 51, 2939–2949. doi:10.1103/PhysRevE.51.2939, arXiv:9412045.

Sumalee, A., Zhong, R.X., Pan, T.L., Szeto, W.Y., 2011. Stochastic cell transmission model (SCTM): A stochastic dynamic traffic model for traffic state surveillance and assignment. Transportation Research Part B: Methodological 45, 507–533. URL: http://dx.doi.org/10.1016/j.trb.2010.09.006, doi:10.1016/j.trb.2010.09.006.

Szeto, W.Y., 2008. Enhanced lagged cell-transmission model for dynamic traffic assignment. Transportation Research Record 2085, 76–85. doi:10.3141/2085-09.

Viti, F., Rinaldi, M., Corman, F., Tampère, C.M., 2014. Assessing partial observability in network sensor location problems. Transportation Research Part B: Methodological 70, 65–89. URL: http://dx.doi.org/10.1016/j.trb.2014.08.002, doi:10.1016/j.trb.2014.08.002.

Zhao, X., Spall, J.C., 2018. A Markovian Framework for Modeling Dynamic Network

Traffic. Proceedings of the American Control Conference 2018-June, 6616–6621. doi:10.23919/ACC.2018.8430861.